RESEARCH PAPER

A Novel Hybrid Multi-Modal Pipeline for Camouflaged NSCLC Detection in Whole-Body PET-CT Imaging

Shruthi N[1], Manju N[1*]
[1]Department of Information Science and Engineering, JSS Science and Technology University, Mysore-570006, Karnataka, India

Email ID: [1]shruthin@jssstuniv.in, [1*] manjun007@jssstuniv.in (Corresponding Author)

ABSTRACT
Lung cancer particularly Non Small Cell Lung Cancer (NSCLC) remains leading cause of cancer mortality worldwide, therefore accurate detection and staging essential for effective treatment. Conventional single-modality approaches often fail in presence of low-contrast and camouflaged tumors, limiting diagnostic reliability. This study presents hybrid multi-modal pipeline for NSCLC tumor detection, classification and staging from whole-body Positron Emission Tomography-Computed Tomography (PET-CT) images. The proposed pipeline integrates six stages i) preprocerssing for noise suppression and lesions visibility improvement. ii) Hybrid Multi-Threshold Segmentation combines Otsu and Yens methods, ensures lung masks and preserve low-intensity tumors. iii) Multi-modal detection by integrating intensity, edge, and texture based analysis. iv) Features extracted based on geometric and intensity to capture tumor morphology and internal appearance variations. v) Weighted camouflage scoring system using seven extracted conditional feature weights identifies NSCLC, blends with surrounding tissue. vi) Automated staging of tumour is efficiently classified into early, intermediate and advanced based on pixel area. Validation on PET-CT images highlights effective preprocessing with PSNR 32.84db, SSIM 0.91 and CNR 4.72. The pipeline achieved robust segmentation performance with Dice 86.42%, IoU 78.93% and Precision 84.68%. The classification outperforms by obtaining Accuracy 82.61% and F1-score 81.39%. Further achieved Staging Accuracy of 79.63%. Overall, the pipeline demonstrates a reliable and clinically applicable solution for NSCLC detection and staging.

Keywords:Non-Small Cell Lung Cancer (NSCLC), Whole- body PET-CT Image, Multi-Modal Pipeline, Camouflaged Tumor, Cancer Staging.
How to cite this article: Shruthi N, Manju N. A Novel Hybrid Multi-Modal Pipeline for Camouflaged NSCLC Detection in Whole-Body PET-CT Imaging. Int J Drug Deliv Technol. 2026;16(59s): 273-284. DOI: 10.25258/ijddt.16.59s.26
Source of support: Nil
Conflict of interest: None

1. INTRODUCTION

Lung cancer considered for about 2.5 million new cases and 1.8 million demises worldwide in 2022, making it one of the leading sources of cancer-related impermanence globally [1]. In Europe alone the number of estimated 237,434 individuals have been lost the lives which assigns to lung cancer in 2024 [2]. Reflecting the global need of precise diagnostic systems, NSCLC accounts for approximately 85% of all lung cancer cases and exhibits significant variability in tumor appearance, location, and growth patterns across patients. Early and accurate identification remains the most effective approaches for improving patient outcomes, as it enables timely intervention and reduces disease progression. The clinical challenges associated with volumetric analysis demand complex solutions in the form of robust, computerized, and interpretable systems capable of detecting NSCLC from clinical data.

While imaging technologies have improved significantly and are being used clinically for NSCLC detection using PET-CT, the existing computational frameworks have concentrated mostly on singal modality approaches [3]. In singal modality approaches, both PET and CT images are analyzed and various methods are utilized to highlight region of interest. For example, strength thresholding has been successfully applied to highlight potential tumor regions in PET-CT images; however, it is not effective when the contrast in the image is below a certain threshold or when the structures at region boundaries camouflaged. Entry-based approaches were among the earliest computational framework solutions developed for automatic detection but they suffered from high false alarm rates and failed to demonstrate clinical suitability [4]. Manual segmentation

and annotation of tumors by radiologists is time consuming and also prone to inter-observer variability which affects patients' treatment decisions. Although there are systems that combine detection, segmentation and classification, most current systems treat as separate sequential tasks or pipeline instead of integrating them as one end-to-end task.

To enhance the accuracy and efficiency of lung cancer diagnosis machine learning and deep learning approaches have been proposed in numerous studies. Recent studies based on deep learning techniques reports state-of-the-art results such as 94.62% accuracy using Vision Transformers and 93.69% accuracy using 3D-CNNs for lung cancer detection [5]. However, existing deep learning approaches such as 3D U-Net, Mask R-CNN, nnU-Net, and Multi-View CNN which require a vast number of annotated datasets and operate as black boxes models [6]. Image preprocessing is a critical step for developing accurate PET-CT based lung cancer detection systems. Detection accuracy and segmentation performance is significantly affected by differences in intensity distribution across images acquired from different scanners [7]. Contrast Limited Adaptive Histogram Equalization (CLAHE), filtering, and lung region extraction techniques were widely used to improve the quality of image visibility of lesion. Improved detection of low-density nodules and enhanced segmentation performance has been demonstrated by experimental studies through appropriate combinations of contrast enhancement, filtering, and intensity windowing techniques [8,10]. Those models still get affected by noise and different protocol changes. Their strong requirement for big annotated datasets is one of the factors limiting their generalization and clinical usefulness. Mostly for small or disguised tumors. Also, it is common to find PET-CT datasets in NSCLC with a heavy imbalance in the number of malignant cases versus the benign ones, which leads to an introduction of the class imbalance problem that lowers the reliability of detection even more. This imbalance is a continuous problem that often causes a decrease in detection accuracy if not handled cautiously during preprocessing.

To address these limitations, a modular six-stage hybrid multi-modal pipeline is developed for NSCLC tumor detection, segmentation, classification and automated staging from whole-body PET-CT images. This proposed pipeline is fully interpretable, efficient and does not require training of a deep neural network. It consists of the following independent modules: i) edge-preserving preprocessing using Contrast-Limited Adaptive History Equalization (CLAHE) and median filtering, ii) hybrid segmentation using Otsu thresholding and Yen thresholding and post-processing by morphological operations, iii) multi-modal detection of NSCLC using intensity, edge and texture information extracted from CT images, iv) extraction of large-scale, spatially adaptive, radiomic features from detected lesions, v) a novel seven factor weighted camouflage probability scoring system for assessment of the likelihood of cancer, and vi) automated pixel area-based tumor staging. The proposed framework provides a unified and interpretable solution encompassing all major stages of NSCLC analysis within a single pipeline.

2. RELATED WORK

PET-CT based NSCLC detection from classical preprocessing and segmentation methods to advanced deep learning and radiomics have been explore by researchers over the decade. However, most studies focus on individual tasks, highlighting the need for unified and clinically interpretable frameworks.

2.1 Preprocessing Techniques for Lung Cancer Detection

Image preparation is one of the most important stages in PET-CT based image analysis and detection methods. The quality of the images directly detrmines the effectiveness of subsequent segmentation and classification operations. A CNN based classification methodologies for lung tumor in PET-CT images, which combines CLAHE as the preliminary preprocessing technique integrated with wavelet transform for feature engineering [9]. The results demonstrates that the CLAHE productively minimizes false positives. By intensifying regional contrast in zones holding low-density nodules that are rather difficult to differentiate from the neighboring parenchymal tissue. The amalgamation of CLAHE with filtrate was manifested to enhance classification effectiveness by defeating noise artifacts, while protecting diagnostically relevant boundary information near tumor regions. An evaluation of preprocessing method combinations CLAHE with Butterworth filtering, DWT with thresholding, CLAHE with median filtering, Median-Mean Hybrid Filtering, and Unsharp Masking with Bilateral Filtering [10]. Median filtering with the combination of CLAHE provides the effective stability balance between noise conquering and edge protection across PET-CT imaging. Noise in adjacent

parenchymal regions is reduced by effectively maintaining tumor border integrity with the validation of the mutual filter for its edge-preserving capability. The results provide strong evidence that the combination of CLAHE and median filtering constitutes a robust preprocessing strategy for PET-CT–based lung tumor classification.

2.2 Lung Tumour Segmentation and Classification Methods

In an extensive review of recent approaches to PET-CT based segmentation, classic approaches, morphological transformations and deep learning-based models were discussed [11]. One of the commonly applied techniques for segmentation is Otsu's thresholding method because of its speed and simplicity. Following thresholding, morphological transformations can be applied to obtain improved lung masks where there is removal of the void regions that form within the lungs due to the inclusion of blood vessels and airways. Variation of the shape, size and intensity of patient lung nodules, and problems with noise in images had to be overcome. One problem with a single thresholding value is its inaccuracy when lung parenchyma is uneven as when in cases with pathologies, like emphysema or pleural effusion. These limitations have driven the adoption of multi-threshold strategies, which deliver more robust and reliable segmentation outcomes. Lung tumour detection, identification, and localization in CT images were carried out by employing multi-level deep learning models and have been tested using 1,608 PET-CT images [12]. Conventional classification models designed to detect and categorize objects in PET-CT images often demonstrate limited effectiveness and tend to underperform. Multi-objective models were more effective when concurrently used for detection, segmentation, and classification, thereby improving both clinical applicability and accuracy.

2.3 Multi-Modal Tumor Detection Strategies

Attention-based deep learning networks along with radiomics features extracted from PET-CT images acquired at multiple healthcare centers [13] incorporates an advanced framework to subtype classification of lung cancer. Accuracy of 85.07% and AUC of 85.98% were achieved by radiomic features that are conventionally extracted using GLCM-derived texture features, with deep CNN features.Non-negative matrix factorization and recursive feature elimination combined with ensemble classifiers XGBoost and Stacking were include in feature selection.The result obtained by multi-modal fusion of intensity-based and texture-based features consistently surpasses single-modality approaches, highlighting the effectiveness of integrating complementary feature information for lung cancer classification.For lung cancer subtype classification [14] an enhanced GraphSAGE framework that combines graph-based deep learning with GLCM feature extraction were used. Tissue inhomogeneity and spatial relationships between tissue regions captured by GLCM-derived texture features, enabling the classification of Adenocarcinoma, Squamous Cell Carcinoma, and Benign Tissue. The results emphasized the fundamental role of GLCM-based texture analysis in distinguishing lung cancer subtypes. Two-stage matrix framework for whole-body PET-CT image acquired DSC 0.70 and sensitivity 0.76. Even these two values have show a big improvement, the problem is far from solved. The most common used methods only adopt the simple intensity thresholding or edge based methods to locate tumor, however, it is no guarantee for tumors whose border is weak or with smooth gradient [15].

2.4 Radiomic Feature Extraction and GLCM-Based Analysis

The effectiveness of radiomic feature diagnosis for accurate detection of lung cancer is investigated thoroughly. This test includes their texture, shape and intensity attribute sets obtained from CT images [16]. The top diagnostic radiomic features are selected based on the analysis of SHAP scores using DenseNet-201 CNN and XGBoost models. GLCM textural features turned out to be the most discriminative radiomic features with success rates above 85% for identifying malignancies. In combination with compact shape attributes, especially surface-to-volume ratio of the object that has been identified as the best morphological descriptor, the classification performance was significantly enhanced to reach up to 88% sensitivity. Therefore, GLCM textural features can be considered a fundamental part of classification algorithms. Tumors were detected against the background of camouflaged lesions, which had nearly identical Standard Uptake Values (SUVs) and texture features compared to their surrounding benign tissues, making them difficult to distinguish using standard segmentation techniques [17]. Despite the evaluated outcomes of the examined metrics, the obtained data suggests that the issue of camouflaged tumors' identification is still open.

2.5 Lung Cancer Staging

The changing role of the imaging techniques, including CT and MRI scans, has been emphasized through the utilization of the imaging parameters in TNM staging of lung cancer patients. Defining imaging parameters has improved accuracy, consistency in staging and clinical decision-making significantly [18]. The proposed TNM staging algorithm with pictorial review that was tested for clinical use showed that imaging guidelines, based on both radiologic findings and pathology, lead to better interpretation, a narrower range of staging variability, and to the clinical necessity of standardized pathways [19-20].

2.6 Research Gap and Motivation

Existing approaches tend to focus on specific parts of the problem, rather than a holistic solution. Preprocessing methods often culminate in classification instead of detection. While the segmentation methods produce accurate lung tumour masks, they ignore the camouflage challenge. Feature-based methods are effective for classification, but they depend largely on deep learning models that lack interpretability. The few attempts at camouflage-specific analysis require on PET-CT images and deliver only modest results. Meanwhile, staging studies confirm the clinical importance of the task but stop short of proposing automated, computerized solutions.

3. METHOD

The proposed six-stage modular pipeline for NSCLC tumor detection is described with its mathematical formulation, parameter setting and implementation.

3.1 Proposed System Architecture

The proposed pipeline illustrates a six-stage modular pipeline which operates systematically from a raw PET-CT image as input to the final tumor staging, as shown in Figure 1. No manual intervention is required between stages. Each stage output feeds directly into the next stage. The six stages are: (i) Image Preprocessing, (ii) hybrid segmentation, (iii) Multi-Modal Tumor Detection, (iv) Feature Extraction, (v) Camouflage Classification and (vi) Automated Staging. The modular design ensures each component can be independently validated without affecting other stages.

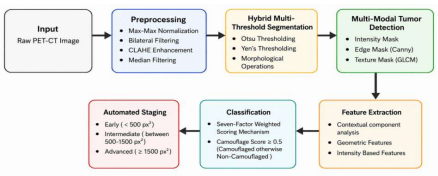

Figure 1. Proposed six-stage modular pipeline architecture for NSCLC tumor detection and staging.

3.2 Dataset Description

The dataset was sourced from the FDG-PET-CT Lesions Collection in TCIA [21], comprising 1,014 whole-body scans, of which 400 histopathologically confirmed NSCLC cases were selected. Expert annotations and real-world artifacts preserved all images in full SUV format, followed by reconstruction at 512 512 resolution with 3-5 mm slice thickness on three different PET-CT systems to reflect clinical variability. Preprocessing mainly focused on standard intensity normalization and isotropic resampling to 1 mm resolution. After that, tumors were categorized as either Camouflaged (low contrast, unsharp boundaries) or non-camouflaged (clear contrast, well-defined boundaries), quantification being the basis for classification, which was facilitated by imaging metrics. The data set was formated as a binary classification problem, and the rule-based approach was tested throughout the entire group of patients without a separate validation set, allowing the method to be evaluated in conditions of realistic clinical imaging.

3.3 Preprocessing

The four-step preprocessing pipeline standardizes raw PET-CT image quality before segmentation.

Step 1: Min-Max normalization standardizes pixel intensity to a uniform [0-255] range across all scanners by using Equation (1).

$$I_{norm}(x,y) = \frac{(I(x,y) - I_{min})}{(I_{max} - I_{min})} \times 255 \quad (1)$$

Where: $I(x,y)$ is a original pixel intensity at position, I_{min} is the minimum intensity value of the image, I_{max} is the maximum intensity value of the image, $I_{norm}(x,y)$ is normalized output intensity in range [0,255].

Step 2: Bilateral filtering reduces noise while preserving tumor boundary edges by using Equation (2).

$$I_{filtered}(x,y) = \frac{1}{W(x,y)} \sum_{w \epsilon \Omega} G_s(||w||) G_r(|I(x+w_x, y+w_y) - I(x,y)| \quad (2)$$

Where: $G_s(w)$ is a spatial Gaussian kernel, G_r is a range Gaussian kernel, w is the filter window neighborhood and $|..|$ is absolute intensity difference.

Step 3: To improve the visibility of low-contrast pulmonary nodules and

camouflaged tumor regions, Contrast Limited Adaptive Histogram Equalization (CLAHE) is applied after bilateral filtering. CLAHE enhances local image contrast by redistributing intensity values within small contextual regions while limiting excessive amplification of noise. The enhancement process is represented in Equation (3).

$$I_{CLAHE}(X,Y) = T_r(I(x,y)) \quad (3)$$

Where: I(x,y) is the input image intensity at pixel location (x,y), Tr represents the adaptive histogram equalization transformation applied within local region r, and I_{CLAHE}(x,y) is the contrast-enhanced output image. Here, CLAHE parameters were set as clipLimit = 3.0 and tileGridSize = (8,8) to improve local tissue visibility while avoiding excessive noise amplification.

Step 4: Following CLAHE enhancement, median filtering is applied as a final smoothing step to remove residual impulse noise and minor artifacts while preserving important tumor boundary structures. A 3×3 kernel is utilized for local neighborhood processing. The filtering operation is expressed in Equation (4).

$$I_{median}(x,y) = \text{median}\{ I(i,j), (i,j)\epsilon N_{3X3}(x,y) \quad (4)$$

Where: $N_{3\times3}$(x,y) denotes the 3×3 neighborhood centered at pixel location (x,y), median{.} represents the median intensity value within the local neighborhood, and Imedian (x,y) is the final smoothed output image used for subsequent hybrid segmentation.

3.4 Hybrid Multi-Threshold Segmentation

Hybrid multi-threshold segmentation integrates otsu's and Yen's methods to produce a complete lung mask under diverse PET-CT imaging conditions. The combined approach helps to preserve anatomically complete pathological regions while reducing the possibility of missing low-intensity areas. Two binary masks were first obtained by using Equation (5) and Equation (6).

$$B_{otsu}(x,y) = \begin{cases} 1 \text{ if } I(x,y) < T_{otsu} \\ 0 \quad \text{otherwise} \end{cases} \quad (5)$$

$$B_{yen}(x,y) = \begin{cases} 1 \text{ if } I(x,y) < T_{yen} \\ 0 \quad \text{otherwise} \end{cases} \quad (6)$$

The two binary masks are fused using a logical OR to capture pathological regions missed by either thresholding methods alone, thereby supporting whole-body tumour localization and spread analysis by using Equation (7).

$$B_{lung}(x,y) = B_{otsu}(x,y) \cup B_{yen}(x,y) \quad (7)$$

Where: B_{lung}(x,y) is initial binary lung mask at pixel coordinates (x,y). To ensure anatomical completeness and suppress spurious regions, sequential morphological operations were applied to B_{lung}(x,y). The refinement pipeline is expressed in Equation (8).

$$M_{lung}(x,y) = \text{opening}(\text{closing}(\text{fillholes}(\text{reomovesmall}(B_{lung}(x,y))))) \quad (8)$$

Where: M_{lung}(x,y) is final refined lung mask at pixel coordinates (x,y). removesmall(□) removes small connected components (noise or spurious regions). fillholes(□) fills internal holes within the binary mask to ensure contiguous lung regions. closing(□) morphological closing (dilation followed by erosion) to close small gaps and smooth boundaries. opening (□) morphological opening (erosion followed by dilation) to remove small protrusions and refine the mask edges.

3.5 Multi-Modal Tumor Detection

A multi-modal tumour detection is implemented by integration of intensity-based, edge-based and texture-based analysis in order to enhance the tumour localization within the segmented pathological region. Joint strategy improves the detection of heterogeneous tumour appearances including low-contrast and high-intensity lesions. The process starts by employing a double-intensity threshold approach on the masked lung image to identify hypointense and hyperintense areas where the presence of tumors is suspected. Because of this, the process ensures that tumors with varied metabolic characteristics can be detected. Edges are then obtained using the Canny Edge Detector algorithm where structural edges relating to areas that might contain tumors are extracted. Prior to this, smoothing is conducted. To further improve edge detection for more accurate segmentations, a dilation process is done to strengthen the edges of the tumor areas. The equation for edge enhancement is shown in Equation (9).

$$M_{edge}(x,y) = \text{dilate}(E(x,y) \cap M_{lung}(x,y)) \quad (9)$$

Where: E(x,y) denotes the detected edge map and M_{lung}(x,y) represents the segmented lung mask.

Texture analysis is used to further examine tissue heterogeneity using the Gray

Level Co-occurrence Matrix (GLCM). Dissimilarity is utilized to detect areas with significant intensity variation since such an area is known to be related to the presence of malignant tissue structures. The texture response is computed as given in Equation (10).

$$M_{text}(x,y) = \sum_{i,j} |i-j|^2 \cdot p(i,j) \quad (10)$$

Where: p(i,j) represents the GLCM probability distribution between neighboring intensity pairs. Regions producing texture responses greater than 0.3 are considered suspicious tumor candidates. Finally, the intensity, edge, and texture responses are integrated through logical OR fusion to generate the final tumor candidate mask used for subsequent feature extraction and camouflage analysis.

3.6 Feature Extraction and Classification

Connected component analysis with 8-connectivity is applied to the fused tumor candidate mask to isolate individual suspicious regions.to reduce noise, small isolated regions and excessively large non-tumor structures are discarded, retaining only those within the range of 50–5000 pixels. For each surviving candidate region, geometric and intensity-based features are extracted to capture tumor morphology and internal appearance variations. Compactness is computed using Equation (11).

$$C_i = \frac{4\pi A_i}{P_i^2} \quad (11)$$

Where: A_i denotes the area of the region and P_i represents its perimeter. Similarly, solidity is estimated using Equation (12).

$$S_i = \frac{A_i}{A_i^{convex}} \quad (12)$$

Where: Ai, convex represents the convex hull area of the corresponding region.

To estimate the likelihood of tumor camouflage within surrounding tissues, a seven-factor weighted scoring mechanism is introduced. The scoring framework integrates intensity, shape, and texture characteristics to quantify camouflage probability. The cumulative camouflage score is computed using Equation (13).

$$P_{camouflaged} = \min(1.0 \sum_{i=1}^{7} W_i \times F_i) \quad (13)$$

Where: W_i represents the assigned feature weight and F_i denotes the normalized feature response.

Tumor regions with camouflage probability greater than 0.5 are classified as camouflaged; otherwise, they are categorized as non-camouflaged, as defined in Equation (14).

$$\text{Class} = \begin{cases} \text{Camouflaged} & \text{if } P_{camouflaged} > 0.5 \\ \text{Non} - \text{Camouflaged} & \text{otherwise} \end{cases} \quad (14)$$

The detailed feature weighting conditions used for camouflage scoring are summarized in Table 1.

Table 1. Camouflage Probability Weight Conditions

Weight	Condition	Value
W_1	Mean Intensity < 150	0.30
W_2	Intensity within [120,160]	0.20
W_3	Solidity < 0.8	0.10
W_4	Eccentricity > 0.7	0.10
W_5	Standard Intensity > 20	0.10
W_6	Area < 500 px²	0.10
W_7	Circularity < 0.6	0.10

3.7 Automated Staging

For each tumor region identified in the images, subsequent camouflage classification will be applied to characterize lesion visibility and representation, each stage of the tumour is assigned based on the pixel area, as given in Equation (15). The three stages are broadly consistent with TNM-inspired tumour size classification and reflect three levels of severity of the disease. T (Tumour) – Size and extent of the primary tumour; N (Node) - Presence of regional lymph node metastasis; M (Metastasis) - Presence of distant metastasis.

$$\text{Stage}(R_i) = \begin{cases} \text{Early if } A_i < 500 \text{ px}^2 \\ \text{Intermediate if } 500 \le A_i < 1500 \text{ px}^2 \\ \text{Advanced if } A_i \ge 1500 \text{ px}^2 \end{cases} \quad (15)$$

Where: Ri represents the detected tumor region and Ai denotes the corresponding tumor area measured in pixels².

4. RESULTS AND DISCUSSION

The Validation of six-stage pipeline has been performed in a thorough experimental manner. Also, the optical outputs of the system have been included along with aggregate analysis to demonstrate its relevancy.

4.1 Evaluation Metrics

For assessing the correctness and consistency of tumor delineation, the performance of the segmentation on the PET-CT dataset was quantified during the

preprocessing step. Five separate measures were used to evaluate the quality of the segmentations based on the accuracy of overlap and the consistency of boundaries. These five-evaluation metrics collectively constitute a complete evaluation of the quality of the classification and staging, which proves the robustness of the proposed model. The evaluation metric and its application in this study are listed in Table 2.

Table 2. Evaluation Metrics Used

Processing Stages	Metric	Formula	Purpose in this work
Preprocessing	PSNR	$PSNR=10\log_{10}$	Measures preprocessing fidelity and noise suppression.
	SSIM	$SSIM(x,y)=\frac{(2}{(\mu_x^2}$	Evaluates structural preservation and perceptual quality.
	CNR	$CNR=\frac{\lvert\mu_{lesion}-\mu_b}{\sigma_{backg}}$	Quantifies lesion visibility improvement.
Segmentation	Dice	$Dice=\frac{2TP}{2TP+FP+}$	Assesses segmentation overlap accuracy.
	IoU	$IoU=\frac{TP}{TP+FP+F}$	Stricter overlap measure for segmentation.
	Sensitivity	$Sensitivity=\frac{T}{TP}$	Ability to correctly identify tumor pixels.
	Specificity	$Specificity=\frac{T}{TN}$	Ability to correctly exclude non-tumor pixels.
	Precision	$Precision=\frac{TP}{TP+}$	Reliability of predicted tumor pixels.
Classification & Staging	Accuracy	$Accuracy=\frac{}{TP+}$	Overall correctness of classification.
	Precision	$Precision=\frac{TP}{TP+}$	Reliability of predicted tumor classifications.
	Recall	$Recall=\frac{TP}{TP+FN}$	Correct identification of camouflaged tumors.
	F1-Score	$F1=\frac{2.Precision.}{Precision+}$	Balanced measure of classification under imbalance.
	Staging Accuracy	$\frac{\text{Correct Stages}}{\text{Total Cases}}$	Measures correctness of automated tumor stage assignment.

4.2 Experimental Results

4.2.1 Preprocessing

Peak Signal-to-Noise Ratio (PSNR), for medical images, a PSNR greater than 40 dB represents an excellent result with no diagnostic loss, a PSNR between 30-40 dB is considered acceptable, and values less than 30 dB represent significant degradation. Structural Similarity Index Measure (SSIM) ensures structural fidelity and values close to 1, which indicate strong structural preservation. Contrast-to-Noise Ratio (CNR) quantifies lesion visibility, which is critical in PET-CT tumor analysis, greater than 4 strong visibility lesion conspicuity is high, clinically robust for tumor detection. The PSNR 32.84dB, SSIM 0.91, and CNR 4.72, demonstrates successful noise suppression, preservation of structure, and improvement in the visibility of lesions. SUV normalization and contrast enhancement resulted in improved images suitable for further accurate analysis of the tumors. Quantitative evaluation of the performance of the preprocessing stage is shown in Figure 2.

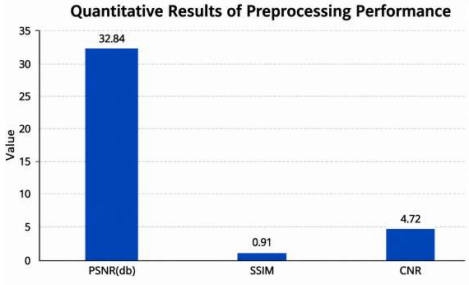

Figure 2. Quantitative Results of Preprocessing Performance

4.2.2 Hybrid Multi-Threshold Segmentation

the proposed segmentation method obtaines the Dice coefficient 86.42%, IoU 78.93%, Sensitivity 91.23%, Specificity 88. 47%, and Precision 84. 68%. The figures reflect very accurate tumor boundary extraction, highly reliable detection performance of various tumor types, and overall high accuracy. Quantitative results of the proposed method's segmentation performance are presented in Figure3.

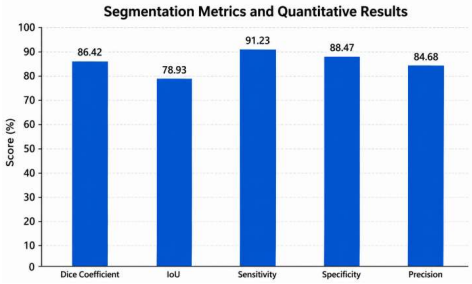

Figure 3. Segmentation Metrics and Quantitative Results

4.2.3 Classification & Staging

The accuracy obtained is 82.61%, precision is 83.42%, recall is 80.34% and F1-score is 81.39% which indicates high reliability in distinguishing low-contrast tumours in camouflage analysis.79.63% accuracy is achieved in staging in this method which shows its capability automatically classify tumours into early,intermediate and advanced stages based on measurements of radiomic-based features and pixel areas. Figure4. Summarizes the results of both classification and staging graphically.

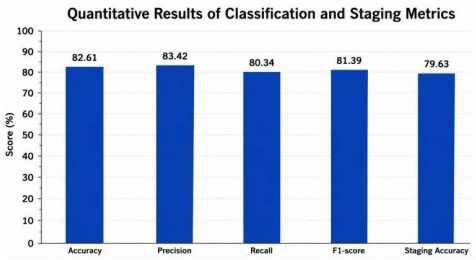

Figure 4. The classification and staging Metrics and Quantitative Results

The pre-processing pipeline on whole-body PET-CT scan consisting of denoising, contrast enhancement and normalization of intensity with respect to SUV. The output of the pre-processing step makes visualization of the lesions and the normalization of metabolic uptake values as shown in Figure 5.

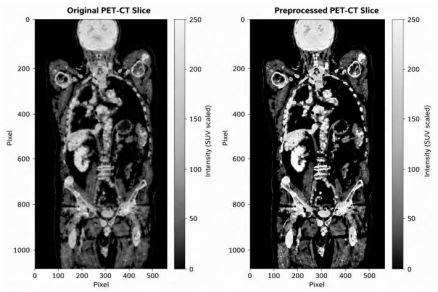

Figure 5. Original and Preprocessed Whole-Body PET-CT Images

Figure 6. presents a sample output from the tumor analysis pipeline, which integrates segmentation, detection, camouflage classification, radiomic feature extraction, and stage assessment. The segmented tumor regions are then classified into early, intermediate, or advanced stages based on quantitative feature profiles and pixel-area measurements.

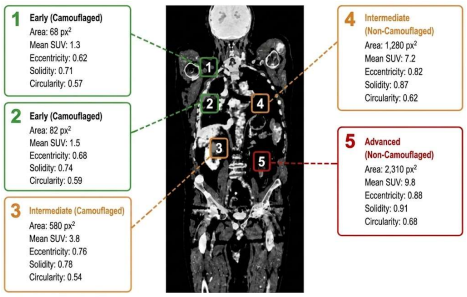

Figure 6. Multi-Stage Tumor Analysis and Staging

4.2.4 Comparison with Baseline Methods

To validate the effectiveness of the proposed approach, comparisons were conducted against five widely adopted benchmark techniques representing different categories of tumor detection and segmentation methodologies. A 3D U-Net architecture was implemented and trained from scratch using the same PET-CT dataset for deep learning-based volumetric tumor segmentation. Mask R-CNN integrated with a ResNet-50 backbone pre-trained on ImageNet was utilized for region-based tumor localization and segmentation. nnU-Net was included as a self-configuring medical image segmentation framework optimized for automated tumor analysis. Additionally, a Multimodal CNN model incorporating orthogonal plane reconstruction was evaluated for pulmonary nodule characterization and classification.

Tables 3 and Table 4 shows that our proposed pipeline achieves higher scores than baseline and stateof-of-the-art methods across segmentation, classification, and staging on the same PET-CT dataset.

Table 3. Quantitative comparison of Segmentation Metrics with recent state-of-the-art method and baseline approaches on the same dataset.

Method	**Dice (%)**	**IoU (%)**	**Sensitivity (%)**	**Specificity (%)**	**Precision (%)**
3D U-Net	78.47	70.12	82.34	85.21	79.63
Mask R-CNN	81.35	73.64	85.08	86.47	82.14
nnU-Net	83.69	75.82	87.63	87.92	83.56
Multi-View CNN	79.76	72.18	83.92	85.63	80.47
Proposed	**86.42**	**78.93**	**91.23**	**88.47**	**84.68**

Method	Dice (%)	IoU (%)	Sensitivity (%)	Specificity (%)	Precision (%)
Pipeline					

Table 4. Quantitative comparison of Classification and Staging Metrics with recent state-of-the-art method and baseline approaches on the same dataset.

Method	Accuracy (%)	Precision (%)	Recall (%)	F1-Score (%)	Staging Accuracy
3D U-Net	77.84	78.92	76.92	78.25	65.18
Mask R-CNN	79.26	80.41	78.41	80.26	71.52
nnU-Net	80.41	81.27	79.12	81.31	74.83
Multi-View CNN	78.63	79.18	77.21	78.91	72.28
Proposed Pipeline	**82.61**	**83.42**	**80.34**	**81.39**	**79.63**

Ablation Study and Computational Analysis

In order to determine the role played by each component of pipeline, selective elimination of modules was performed. The results emphasize the significance of texture analysis, edge detection, thresholding intensity, and camouflaging scores on segmentation accuracy and classification reliability. As summarized in Table 5, comparative outcomes across Dice, Sensitivity, and Accuracy confirm that each stage plays a significant role in driving overall system performance.

Table 5. Ablation Study of pipeline Components

Configuration	Dice (%)	Sensitivity (%)	Accuracy (%)	Interpretation
Single-Threshold Segmentation	82.28	86.19	78.91	Highlights superiority of unified multi-threshold approach for robust segmentation and classification.
Without Camouflage Scoring	84.09	88.71	80.87	Slight sensitivity reduction; demonstrates contribution to low-contrast tumor detection and staging accuracy.
Without Intensity Thresholding	79.41	83.12	77.23	Confirms hybrid Otsu–Yen fusion improves lesion isolation and classification fidelity.
Without Edge Detection	81.68	85.32	78.39	Reduced boundary precision; validates edge-based localization importance.
Without Texture Analysis	83.17	87.46	79.82	Largest drop; confirms radiomic texture features enhance lesion discrimination and classification.
Proposed Pipeline	**86.42**	**91.23**	**82.61**	Optimal segmentation overlap accuracy, high lesion detection sensitivity, and reliable classification correctness

Discussion

The proposed pipeline reported good performance of sensitivity and Dice score to 91.23% and 86.42% respectively which implies the performance of the pipeline is good for NSCLC lesion segmentation and detection. Tumors masked in normal lung tissues discovered by framework with the help of the intensity, edge and texture. Lung masks that are completer and more reliable by the hybrid Otsu-Yen segmentation. Despite these encouraging outcomes, certain limitations remain. The current implementation processes 2D image slices, limiting its ability to capture full 3D tumor morphology. Moreover, the staging approach, based on pixel area, does not correspond directly to formal TNM clinical staging. Validation was conducted on a relatively small PET-CT dataset, and broader multi-center studies are needed to confirm generalizability.

5. CONCLUSION

The proposed multi-model framework highlights a reliable and effective approach for automated NSCLC classification and staging from whole-body PET-CT images. Achieved by integrating advanced preprocessing, hybrid multi-threshold segmentation, multi-modal feature analysis, and weighted camouflage assessment. The pipeline successfully addresses the limitations of conventional single-modality techniques, particularly in detecting low-contrast and visually concealed tumors. The experimental outcomes confirm substantial improvements in image enhancement,robust segmentation, classification, and clinical diagnostic staging when compared with established state-of-the-art baseline models. The capability of the proposed system to preserve structural information while accurately identifying complex tumor patterns. Proposed method highlights its potential aid for clinical decision-making in oncology imaging. Therefore, the pipeline establishes a promising foundation for developing intelligent and clinically adaptable PET-CT analysis systems for early and reliable NSCLC detection. Future work will focus on extending the pipeline to 3D volumetric analysis, refining the camouflage scoring mechanism, and integrating the system with clinical PACS environments for real-world deployment.

FUNDING INFORMATION

Authors state no funding involved.

AUTHOR CONTRIBUTIONS STATEMENT

Shruthi N: Conceptualization, methodology, software, formal analysis, visualization, writing-original draft.

Manju N: Supervision, validation, review and editing, project administration.

CONFLICT OF INTEREST STATEMENT

The authors declare no conflict of interest.

DATA AVAILABILITY

A whole-body FDG-PET/CT dataset with manually annotated tumor lesions (FDG-PET-CT-Lesions). The Cancer Imaging Archive, 2022, https://doi.org/10.7937/GKR0-XV29.

REFERENCES

[1] T. B. Kratzer, P. Bandi, N. D. Freedman, R. A. Smith, W. D. Travis, A. Jemal, and R. L. Siegel, "Lung cancer statistics, 2023",Cancer, Vol. 130, No. 5, pp. 1330–1348, 2024.

[2] C. Santucci, S. Mignozzi, M. Malvezzi, P. Boffetta, G. Collatuzzo, F. Levi, C. La Vecchia, and E. Negri, "European cancer mortality predictions for the year 2024 with focus on colorectal cancer", Annals of Oncology, Vol. 35, pp. 308–316, 2024.

[3] D. Rawat, S. Sharma, and S. Bhadula, "CT imaging-based deep learning system for non-small cell lung cancer detection and classification", International Journal of Advanced Computer Science and Applications, Vol. 16, No. 5, 2025.

[4] Z. Lu, X. Li, S. Gao, R. Tan, and Y. Liu, "Research progress in computer-aided diagnosis systems for lung cancer", npj Digital Medicine, Vol. 8, No. 1, 2025.

[5] V. Shariff, C. Paritala, and K. M. Ankala, "Optimizing non-small cell lung cancer detection with convolutional neural networks and differential augmentation", Scientific Reports, Vol. 15, p. 15640, 2025.

[6] S. Mahanta, R. Das, and P. Nath, "Emerging computational intelligence-based techniques for lung cancer diagnosis and classification on chest CT scan images: a comprehensive survey", Artificial Intelligence Review, Springer Nature, 2026.

[7] N. Nagaraj, R. Krishnan, and S. Patel, "Multi-phase deep learning framework with multiscale adaptive swin transformer and embedding attention for precision lung nodule detection and classification", Scientific Reports, Vol. 15, 2025.

[8] F. Muñoz-Montoya, J. Vera-Candeas, and M. Cañadas-Quesada, "Statistical analysis of nnU-Net models for lung nodule segmentation", PMC — MDPI, 2024.

[9] F. Moreira, A. Silva, and R. Costa, "Classification of lung cancer in medical imaging using convolutional networks with CLAHE preprocessing and wavelet transform", ResearchGate, 2025.

[10] M. Alfargose, K. Ahmed, and T. Hassan, "Evaluating pre-processing and deep learning methods in medical imaging: combined effectiveness across multiple modalities", Biomedical Signal Processing and Control, ScienceDirect, 2025.

[11] K. Sivaramakrishnan, G. Murugan, and P. Chen, "Lung tumor segmentation: a review of the state of the art", Frontiers in Computer Science, Vol. 6, 2024.

[12] G. Kasinathan, S. Jayakumar, A. K. Bishoyi, and A. Yadav, "Multi-objective deep learning for lung cancer detection in CT images: enhancements in tumor classification, localization and diagnostic efficiency", Discover Oncology, Vol. 16, p. 529, 2025.

[13] M. Alsallal, H. H. Ahmed, R. A. Kareem, and A. Omar, "Enhanced lung cancer subtype classification using attention-integrated DeepCNN and radiomic features from CT images: a focus on feature reproducibility", Discover Oncology, Vol. 16, p. 336, 2025.

[14] I. Dad, J. He, and Z. Baloch, "Graph-based analysis of histopathological images for lung cancer classification using GLCM features and enhanced graph", Frontiers in Oncology, Vol. 15, p. 1546635, 2025.

[15] Y. He, Z. Wang, K. Fang, and T. Su, "Whole-body tumor segmentation from PET/CT images using a two-stage cascaded neural network with camouflaged object detection

mechanisms", Medical Physics, Vol. 50, pp. 4191–4203, 2023.

[16] N. Alshehri, K. Ahmed, and R. Patel, "Uncovering the diagnostic power of radiomic feature significance in automated lung cancer detection: an integrative analysis of texture, shape and intensity contributions", Diagnostics, Vol. 4, No. 4, p. 129, MDPI, 2024.

[17] J. Paramasamy, S. Mandal, M. Blomjous, D. Bos, and J. G. J. V. Aerts, "Validation of a commercially available CAD-system for lung nodule detection and characterization using CT-scans", European Radiology, Vol. 35, pp. 1076–1088, 2025.

[18] M. R. Chappidi, A. S. Purysko, and A. C. Westphalen, "Imaging of lung cancer staging: TNM 9 updates", Seminars in Ultrasound, CT and MRI, Vol. 46, No. 1, pp. 83–89, 2025.

[19] R. Rami-Porta, A. Nicholson, and W. D. Travis, "Clinical TNM lung cancer staging: a diagnostic algorithm with a pictorial review", Diagnostics, Vol. 15, No. 7, p. 908, MDPI, 2025.

[20] M. A. Baqir, S. Qayyum, N. Ashfaq, and W. Malik, "A lightweight CNN for enhanced non-small cell lung cancer classification using CT scan image", Scientific Reports, 2026.

[21] S. Gatidis and T. Kuestner, "A whole-body FDG-PET/CT dataset with manually annotated tumor lesions (FDG-PET-CT-Lesions)." The Cancer Imaging Archive, 2022, https://doi.org/10.7937/GKR0-XV29.

BIOGRAPHIES OF AUTHORS

Shruthi N received the B.E. degree in Information Science and Engineering from Maharaja Institute of Technology, Mysore, India, in 2011, and the M.Tech. degree in Software Engineering from Sri Jayachamarajendra College of Engineering (SJCE), Mysuru, India, in 2015, both affiliated with Visvesvaraya Technological University (VTU), Belagavi, India. She is currently pursuing doctoral research in the area of artificial intelligence–enabled medical image analysis and serves as an Assistant Professor with the Department of Information Science and Engineering, JSS Science and Technology University (JSS STU), Mysuru, India. Her research interests encompass medical image computing, machine learning, deep learning, computer vision, image processing, and intelligent healthcare systems. Shruthi N has authored and co-authored several research articles published in reputed international journals and conference proceedings. She is the inventor of a published innovation (utility) patent entitled "Camouflaged Lung Tumor Detection and Staging in Whole-Body PET-CT Images Using Object Detection and Learning Models." Her research contributions aim to bridge the gap between artificial intelligence and clinical decision support systems for precision oncology and computer-aided diagnosis. She is a Life Member of the Indian Society for Technical Education (ISTE) and The Institution of Engineers (India) [IEI]. Her long-term research vision is to develop robust, interpretable, and clinically deployable AI frameworks for next-generation healthcare applications.

	ORCID iD: 0000-0003-1576-8664 | Scopus Author ID: 59933966900 | Web of Science ResearcherID: QIU-3509-2026
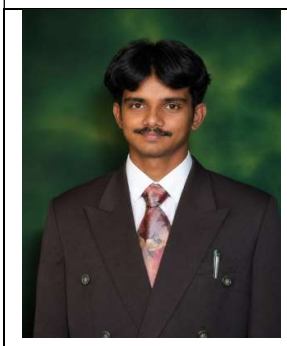	**Dr. Manju N** obtained his B.E. degree in Computer Science and Engineering from Sri Jayachamarajendra College of Engineering (SJCE), Mysuru, India, followed by an M.Tech. degree in Computer Network Engineering from the National Institute of Engineering (NIE), Mysuru, India. He earned his Ph.D. degree from Visvesvaraya Technological University (VTU), Belagavi, India. He is currently serving as an Associate Professor in the Department of Information Science and Engineering at JSS Science and Technology University (JSS STU), Mysuru, India. He has published several research articles in peer-reviewed international journals and conference proceedings and holds a patent in his area of research. Dr. Manju N has actively contributed to the academic and research community as a reviewer for various international journals and conferences. He has served as a Technical Program Committee (TPC) member and chaired technical sessions at numerous international conferences. In addition, he has been a jury member for several academic and technical events. He has organized and coordinated numerous Workshops, Faculty Development Programs (FDPs), and Invited Talks. He has also served as an external member of the Board of Examinations (BoE) and Board of Studies (BoS) for various academic institutions. He is a Life Member of the Indian Society for Technical Education (ISTE). His research interests include Machine Learning, Computational Intelligence, Image Processing, Computer Networks, and Intelligent Systems. ORCID iD: 0000-0002-6810-8857 | Scopus Author ID: 57113538200 | Web of Science ResearcherID: AAZ-8004-2021